Research Article

Abhinav Singh, Sharanagouda Hiregoudar, Ritika Chauhan, Ajit Varma, Ram Prasad*, and Arti Goel*

Deciphering the synergistic potential of mycogenic zinc oxide nanoparticles and bio-slurry formulation on phenology and physiology of *Vigna radiata*

https://doi.org/10.1515/ntrev-2023-0217
received December 8, 2023; accepted February 9, 2024

Abstract: Nanobiofertilizers have emerged as an innovative tool for enhancing crop productivity. In the current research, zinc oxide nanoparticles (ZnONPs) were mycosynthesized using cell-free supernatant of *Trichoderma harzianum* and optimized for physical parameters. Characterization using UV-Visible spectroscopy, dynamic light scattering analysis, zeta potential analysis, X-ray diffraction (XRD) analysis, Fourier transform infrared spectroscopy (FTIR), Scanning electron microscopy-EDX, and HR-Transmission electron microscopy confirmed the formation of ZnONPs with flower-like morphology and average size of 314 nm. The average zeta potential value of the ZnONPs was +1.9 mV indicating the formation of neutral NPs. FTIR peak at 401 cm^{-1} revealed the presence of ZnONPs. XRD analysis confirmed the hexagonal wurtzite crystalline nature of the ZnONPs. The effect of ZnONPs at 10–1,000 ppm combined with liquid bio-slurry (BS) was studied on seed germination and growth of *Vigna radiata.* Combination of 250 ppm ZnONPs and BS at 1:2 ratio showed 22.6% increase in shoot length as well as 18.4% increase in root length as compared to control in *in vitro* studies. *In Vivo* pot experiments showed no significant difference in secondary metabolites after 60 days, but the root length increased by 38.9% and shoot length increased by 46.95% compared to the control.

*** Corresponding author: Ram Prasad**, Department of Botany, Mahatma Gandhi Central University, Motihari, Bihar, 845801, India, e-mail: rpjnu2001@gmail.com
*** Corresponding author: Arti Goel,** Amity Institute of Microbial Technology, Amity University, Noida, 201301, India, e-mail: agoel2@amity.edu
Abhinav Singh, **Ritika Chauhan**, **Ajit Varma:** Amity Institute of Microbial Technology, Amity University, Noida, 201301, India
Sharanagouda Hiregoudar: Centre for Nanotechnology, University of Agricultural Sciences, Raichur, 584104, India

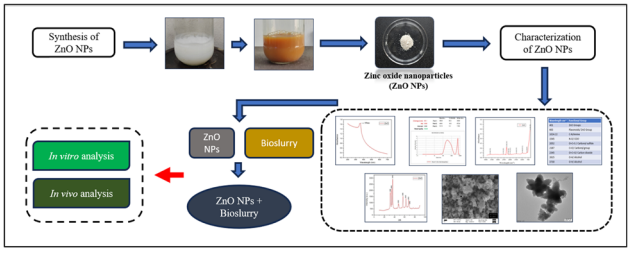

Graphical abstract

Keywords: nanotechnology, agriculture, nanoparticles, bio-slurry, *Vigna radiata*, seed germination

1 Introduction

Legumes are valued worldwide as a sustainable and efficient meat alternative and are considered as the second most important food source after cereals [1,2]. Legumes are nutritionally rich with multiple antioxidants [3] and thus are the savor of many human disorders like hypocholesterolemia, antiatherogenic, anticarcinogenic, and hypoglycemic properties. Legumes have the potential to serve as the foundation for creating various functional foods that can improve human health. Sustainable soil quality improvement is among the top priority problem in the era of climate change [4]. Organic fertilizer sources can address crop and soil quality as well as fertility issues of crops. The reliance on inorganic fertilizers should be reduced because of their high cost, greenhouse gas emissions, and inefficiencies from improper application. Upgrading conventional agricultural practices involves implementation of modern techniques like nanotechnology. Nanoparticles (NPs) can enhance agriculture through precisely targeted delivery of nutrients and crop protection chemicals leading to increased yields and less environmental impact in a highly efficient manner [5]. Alternatively, zinc oxide nanoparticles (ZnONps) in raw bio-

slurry (BS) can escape the threat of using inorganic fertilizers and promote microbial species. There are little data available for the optimal use of BS. Relying solely on chemical fertilizers is not advised, especially for small-scale farmers who have the choice to use organic fertilizer sources. Unlike chemical fertilizers, organic fertilizers release nutrients gradually over time. Optimizing the combined use of ZnONPs and BS has been considered to be a better option to balance high productivity and environmental sustainability [6] as well as can restore the fertility of the soil. BS combination with synthetic fertilizers has been of use as a general fertilizer. But excessive use of chemical fertilizers leads to infertility and toxicity in soil. Therefore, as per the literature, fertilizers formulated through the latest biological trends like nanobiotechnology have come into great existence [7]. Quality is an integral characteristic of marketing products. Increased consumer consciousness of legumes' nutritional and health benefits has led to escalating market demand for them worldwide. It depends on shoot biomass, leghemoglobin and chlorophyll contents, seed protein, nodule numbers, *etc.* Treatment of soil with BS and ZnONPs can affect the aforementioned parameters for the maximum output. The application of mycogenic NPs in combination with BS can have positive impacts on soil microflora by enhancing nutrient availability, detoxifying chemicals, stimulating microbial growth, and increasing enzymatic activity, soil aeration, and water retention, thereby enabling bioremediation. At low concentrations, NPs provide anti-microbial effects but at higher concentrations, this combination can also stimulate growth of beneficial bacteria, fungi, and actinomycetes [8]. BS also leads to carbon sequestration in soil [9].

Research suggests that the use of BS and NPs [10] can also help in the remediation of soil by lowering the cadmium, palladium, and chromium concentrations in soil [11]. Different nanomaterials and combinations of BS have been used for yield enhancement [12]. BS improves the contents of soil by enhancing N, P, and K contents as compared to the modern and conventional methods [13]. The effect of BS and chemical fertilizer on the agronomic performances of maize has been studied in several research papers. One study found that the application of biofertilizer in combination with chemical fertilizer did not significantly alter the levels of dry matter, crude protein, and nitrogen in maize plants [14]. Another study showed that the use of biological nitrogenous fertilizers, such as *Azotobacter* and *Nitrokara*, in combination with chemical nitrogenous fertilizer had a positive effect on plant height, leaf area index, and total dry matter in corn fields [15]. According to a study published, the application of biogas slurry, organic acid, and biofertilizer mixture can significantly alleviate plant growth parameters [16]. Very less data are available on the impact of application and combined usage of BS and NPs on soil health and plant development. Further research needs to be done to unveil the research gaps and the actual mechanism underlying the effects of such formulations and their pathways in plant systems [4].

The current work pioneers an innovative nanotechnology-enabled biofertilizer combining fungal-synthesized ZnONPs and biogas plant slurry to boost *Vigna radiata*'s phenological as well as physiological parameters, representing a significant advancement in sustainable agriculture.

2 Materials and methods

2.1 Chemicals and reagents

Zinc acetate dihydrate [$Zn(CH_3COO)_2{\cdot}2H_2O$] was purchased from SRL Chemicals (India Pvt. Ltd). Potato dextrose agar (PDA) and potato dextrose broth (PDB) were purchased from Hi Media laboratory Pvt. Ltd. All chemicals and reagents used in this study were of laboratory grade. The seeds of *Vigna radiata* (Mh-421) were obtained from Central Arid Zone Institute, Jodhpur, India. BS was obtained from Spectrum Renewable Energy Pvt. Ltd, Rohtak, Haryana. Soil was obtained from Amity University, Noida Campus. Sterilized distilled water was utilized for all the experiments conducted in the current study.

2.2 Maintenance and procurement of fungal culture

Trichoderma harzianum (Indian Type Culture Collection – 7338) was purchased from the Division of Plant Pathology, ICAR-Indian Agricultural Research Institute, New Delhi, India. The fungal culture was sub-cultured on PDA and kept at ±28°C for 7 days. The uniform discs of *Trichoderma harzianum* from 7 days old grown culture were cut with a flame sterilized cork borer (6 mm diameter) and inoculated into a conical flask containing PDB medium [17].

2.3 Preparation of fungal cell-free supernatant

The fungal culture of *Trichoderma harzianum* was sub-cultured on PDA and kept at ± 28°C for 7 days in the Petri

plate. PDB was autoclaved and after cooling the medium, the spores (1×10^8 spores/mL) of *Trichoderma harzianum* were inoculated and the conical flask was kept in the growth chamber at ±28°C for 7–15 days. The pH of the medium was maintained around 7. After the fungal growth, the culture supernatant was separated with Whatman No.1 filter paper and was stored at 4°C for further use [18,19].

2.4 Synthesis of ZnONPs

For the synthesis of ZnONPs, 50 mL cell free culture filtrate of *Trichoderma harzianum* [20] was mixed with 50 mL of 100 mM zinc acetate dihydrate solution [$Zn(CH_3COO_2).2H_2O$]. The pH of the reaction mixture was maintained at around 12. The reaction mixture contained the filtered extract of the fungus *Trichoderma harzianum* and zinc acetate dihydrate solution in a 1:1 ratio. The mixture was heated and stirred at 95°C for 45 min, during which color change was observed indicating NPs synthesis. After observing the color change and NPs precipitation in the main reaction mixture, it was centrifuged at 8,000 rpm for 10 min to separate the NPs from the reaction mixture. The NPs pellet was then washed with deionized water and oven dried overnight at 60°C (Figures 1a–d). Finally, the dried ZnONPs powder was collected and stored in sealed vials at room temperature for later use [21].

2.5 Characterization of mycogenic ZnONPs

ZnONPs have attained significant research interest due to their unique optical, electrical, and magnetic properties that differ from bulk ZnO material. However, the properties of ZnONPs are highly dependent on their morphology, size, crystallinity, and surface characteristics [22]. Therefore, a wide variety of analytical techniques are utilized to fully characterize the structural, compositional, optical, and other relevant properties of ZnONPs. Important techniques like X-ray diffraction (XRD) have been done to determine the crystal structure, electron microscopy to visualize size and even morphology, UV-Visible (UV-Vis) spectroscopy to analyze optical properties, Fourier transform infrared spectroscopy (FTIR) to identify chemical bonding, zeta potential measurements for surface charge *etc.* The current analysis done provides complete information about the fundamental, physical, chemical, and functional properties of the nanoscale ZnO particles.

2.5.1 UV-Vis spectroscopy

The initial analysis of the synthesized ZnONPs was performed using a UV-Vis spectrophotometer (Shimadzu UV-1800) in the 200–800 nm range. For UV-Vis characterization, 100 mg of ZnONPs were suspended in 10 mL of sterile distilled water. ZnONPs exhibit an absorption peak in the UV region that is due to electron transitions from the valence band to the conduction band rather than plasmonic resonance seen in metals [23].

2.5.2 DLS analysis and zeta potential analysis

The average diameter size and zeta potential of the mycosynthesized ZnONPs were analyzed by dynamic light scattering (DLS) using a Malvern ZetaSizer Nano ZS90 instrument. NPs size measurements were performed on 0.1 wt% dispersions of the nanopowder in sterile distilled water, sonicated at 80°C for 4 h. Triplicate measurements were obtained, with 100 runs per measurement at a temperature of 25°C [24].

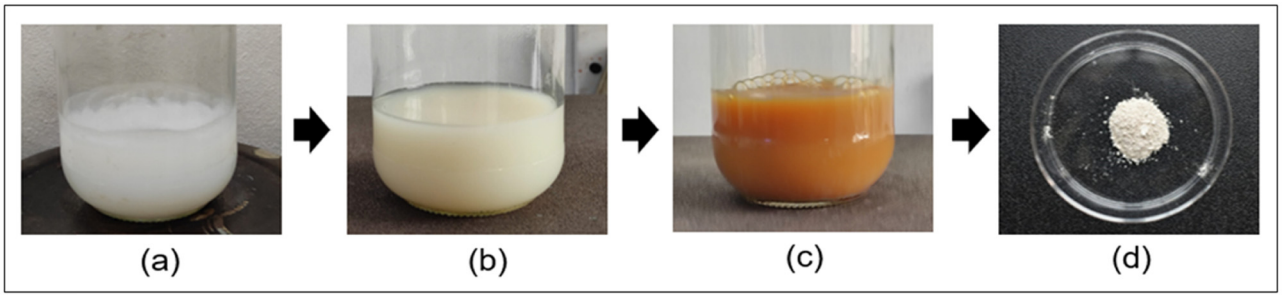

Figure 1: (a) Precursor salt (zinc acetate dihydrate), (b) intermediate reaction mixture (precursor salt and fungal filtrate), (c) NPs formation (visible color change), and (d) synthesized ZnO nanopowder.

2.5.3 FTIR

For FTIR analysis, ZnONPs sample was ground into pellets with KBr powder. The resulting spectra was recorded over the range of 4,000–500 cm^{-1}. This allowed the identification of functional groups present in the NPs for the identification of surface functional groups like C═O, C–H, and O–H based on the peaks from surface coatings or capping agents involved in the synthesis of NPs. FTIR provides critical information about the chemical composition, structure, and functionalization of ZnONPs through the absorption spectrum [25].

2.5.4 XRD

ZnONPs powder was spread on a glass substrate for XRD analysis to determine the crystal structure. The measurements were performed using a Rigaku Ultima-IV X-ray diffractometer over a 2θ angular range of 5°–50°. The Debye–Scherrer equation was utilized to calculate the NPs size from the XRD data. This equation relates the broadening of XRD peaks to the mean crystalline size, based on the principle that smaller NPs produce broader diffraction peaks due to destructive interference effects [26].

2.5.5 Scanning electron microscopy (SEM)

The morphology and size of the synthesized ZnONPs were characterized using SEM on a Zeiss Evo 18 instrument. ImageJ software was utilized to determine the average particle size by taking random measurements of individually dispersed NPs in the SEM micrographs [27].

2.5.6 Transmission electron microscopy (TEM)

An investigation into the dimensions and morphology of the synthesized ZnONPs was conducted utilizing TEM. Imaging was performed on a JEOL JEM-2100 plus instrument operating at an accelerating potential of 50 kV. This provided ultrahigh resolution down to 0.2 Å. Samples were prepared by placing a droplet of the NPs solution onto a copper grid coated with a carbon film. The solvent was allowed to fully evaporate, leaving the NPs dispersed on the grid surface. Multiple micrographs were obtained at random locations on the grid. These images were processed and analyzed using ImageJ particle analysis software to determine the mean particle diameter [28].

2.6 *In vitro* study of different formulation of ZnONPs and BS on *Vigna radiata*

In preparation for the experiments, mung bean (Vigna radiata) seeds were first pretreated to remove surface contaminants. The seeds were immersed in a 10% (v/v) sodium hypochlorite solution for 10 min followed by comprehensive rinsing with distilled water. The treatment with diluted bleach sterilized the seeds and eliminated dust particulates. After this cleaning procedure, the mung bean seeds were utilized immediately for the subsequent experimental steps. Different concentrations of synthesized ZnONPs were then prepared (0, 10, 50, 100, 200, 250, 500, 1,000 mg L^{-1}) in sterile distilled water. 1:2 ratio of ZnONPs and liquid BS was used as a formulation [29].

Eight different treatments were established:

(1) Control plants (C) without any formulation (F)
(2) F1 – BS with 1,000 ppm of ZnONPs
(3) F2 – BS with 500 ppm of ZnONPs
(4) F3 – BS with 250 ppm of ZnONPs
(5) F4 – BS with 200 ppm of ZnONPs
(6) F5 – BS with 100 ppm of ZnONPs
(7) F6 – BS with 50 ppm of ZnONPs
(8) F7 – BS with 10 ppm of ZnONPs.

The seeds were first soaked overnight at room temperature in the different formulations. Seeds were kept for germination in the Petri dishes containing blotting paper wetted with different concentrations of BS and ZnONPs [30]. Later 1 mL of different liquids were added for treatments. A significant control was also maintained. The moisture level in the Petri dishes was kept optimal by adding the concerned combined liquid solution as needed throughout the experiment. Once germination was completed in the Petri plate setup, the root length, shoot length and number of nodules were analyzed and evaluated [31].

2.7 *In vivo* pot studies of different formulations of ZnONPs and BS on *Vigna radiata*

A pot experiment was carried out in the agricultural area of Amity University, Noida, India, to evaluate the effect of formulation of ZnONPs and BS on phonological and physiological parameters of *Vigna radiata* [32]. Eight different treatments were established as discussed in Section 2.6.

2.8 Phenological parameters

To measure the various plant growth parameters plants were taken out from the pots at 30 and 60 days after sowing in three replicates across the treatments. To get rid of the unwanted debris, uprooted plants were carefully cleaned with water having EDTA in it. The plants were cleaned before being laid out in a dark cloth to measure the lengths of the shoots and roots with a standard measuring scale [33].

2.9 Photosynthetic pigment analysis

For the chlorophyll estimation, 0.1 g of fresh leaves were homogenized in 7 mL of dimethyl sulfoxide (DMSO) and incubated in water bath for 30 min at 65°C until color changes from green to white. Then, the homogenate was filtered and total volume was adjusted to 10 mL by adding DMSO. Obtained supernatant was vortexed and was taken for the estimation of chlorophyll a and b absorbance at 645 and 663 nm, respectively [34]. The chlorophyll content (Chl a + Chl b) was calculated using Arnon, 1949. Results were expressed in µg/mL of extract.

$$\text{Chl a} = [0.0127 \times (663\ \text{nm}) - 0.00269 \times (645\ \text{nm})],$$

$$\text{Chl b} = [0.0229 \times (645\ \text{nm}) - 0.00468 \times (663\ \text{nm})].$$

2.10 Estimation of phenolic and flavonoid content

The total phenolic content of plant extracts was determined through the Folin–Ciocalteu colorimetric method by Singleton & Rossi (1965) with slight modifications. The total phenolic content of the plant extracts was then quantified against the gallic acid standard curve and expressed as milligrams of gallic acid equivalents per gram of extract. The analysis was performed in triplicate for each sample to ensure reproducibility. This colorimetric method allows for a simple and rapid determination of total phenolics in plant extracts.

The total flavonoid content in various plant extracts was determined through a colorimetric method using aluminum chloride. For quantification, a standard curve was prepared using quercetin as a reference compound. The flavonoid levels in different plant extracts were expressed in terms of milligrams of quercetin equivalent per gram of extract. This aluminum chloride colorimetric method provides a simple, rapid, and reliable estimation of the total flavonoid content in the plant samples [35].

2.11 Statistical analysis

All the experiments were conducted in triplicates. The values represent mean values ± standard deviation (SD) for three samples in each group. The graphs were graphically presented using excel. All the variables under investigation were subjected to statistical analysis.

3 Results and discussion

3.1 Visual observation and UV-Vis spectrophotometric analysis of mycogenic ZnONPs

In the mycogenic synthesis of ZnONPs using Trichoderma harzianum filtrate, the formation of ZnONPs was primarily monitored by observing color change in the reaction mixture. Specifically, the combination of 100 mM zinc acetate dihydrate and fungal filtrate initially appeared yellowish white but turned brownish over the course of the reaction [36]. This color change to brown indicates the reduction of Zn^{+2} ions to ZnONPs caused by surface plasmon resonance of conduction band electrons on the NPs surface. UV-Visible absorption spectra of the reaction mixture was taken over time demonstrating the emergence of a surface plasmon peak at around 385 nm after 45 min confirming ZnONPs synthesis (Figure 2a) [28]. The surface plasmon resonance wavelength depends upon factors like particle shape, size, composition, dispersion, surface properties, and local environment [37].

3.2 DLS with zeta potential analysis

DLS studies denote the hydrodynamic size of NPs by detecting the random fluctuations in the intensity of light scattered from a suspension. At pH 12, the *Z* average size of ZnONPs was at 499.1 nm and two peaks of ZnONPs were observed: one major peak representing small-sized NPs of size 499.9 nm with 83.3% intensity and another peak representing large-sized particles of 4,918 nm with 16.3% intensity (Figure 2b). Furthermore, the polydispersity index was 0.668 showing the presence of poly dispersed ZnONPs. The neutral nature of the NPs was confirmed by its zeta potential measurement of +1.30 mV with 64.5% intensity (Figure 2c).

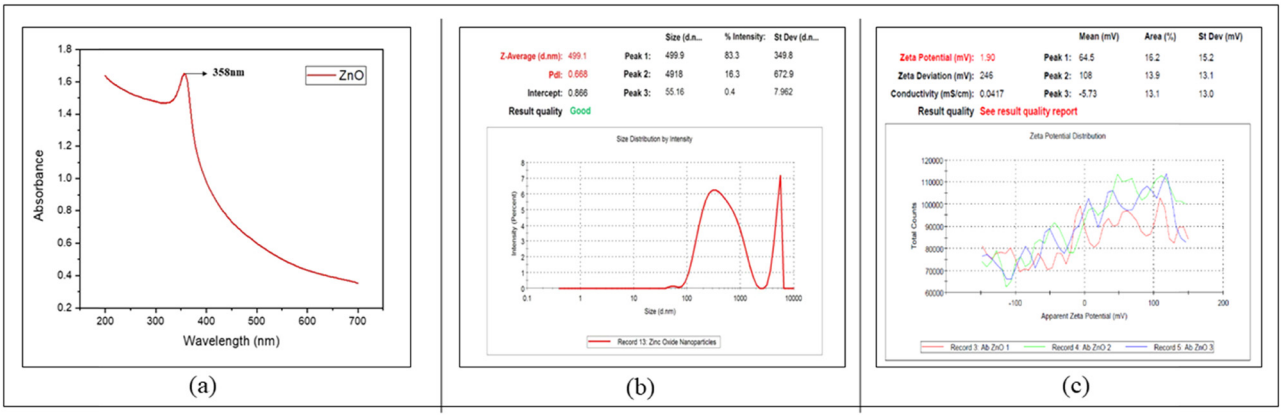

Figure 2: (a) UV-Vis analysis, (b) DLS, and (c) zeta potential analysis of mycogenic ZnONPs.

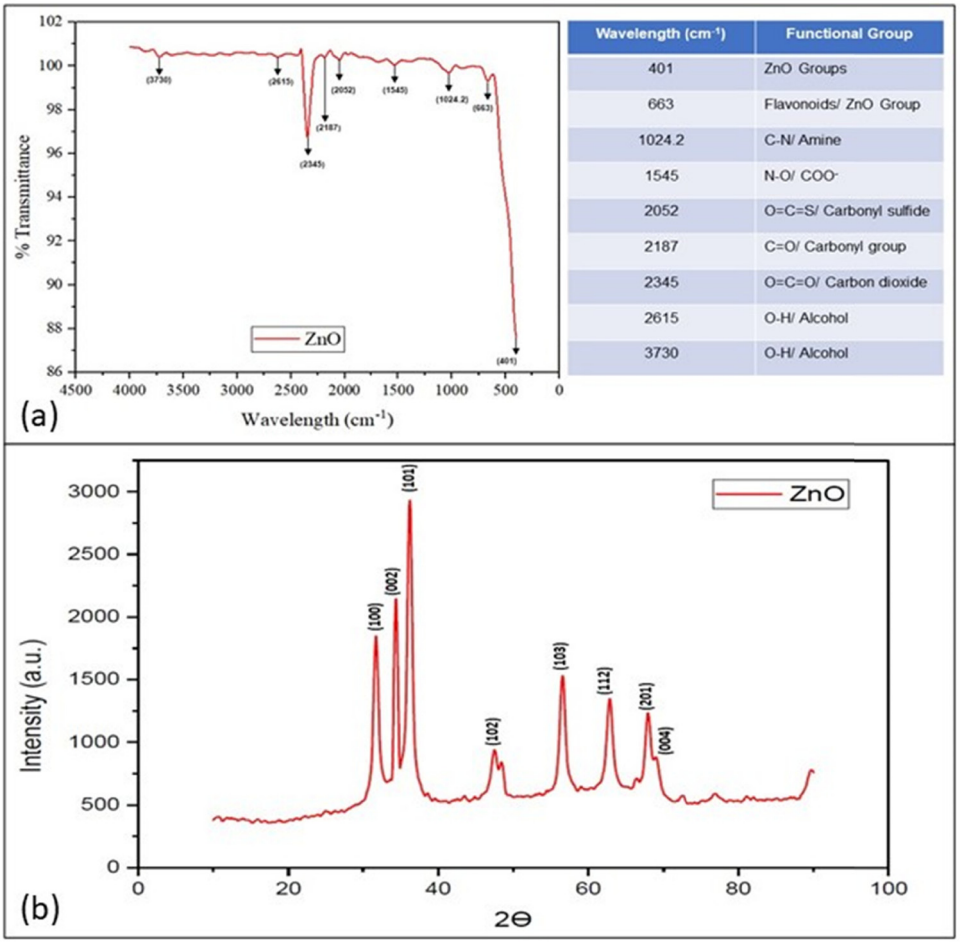

Wavelength (cm⁻¹)	Functional Group
401	ZnO Groups
663	Flavonoids/ ZnO Group
1024.2	C-N/ Amine
1545	N-O/ COO^-
2052	O=C=S/ Carbonyl sulfide
2187	C=O/ Carbonyl group
2345	O=C=O/ Carbon dioxide
2615	O-H/ Alcohol
3730	O-H/ Alcohol

Figure 3: (a) FTIR analysis and (b) powder XRD pattern of mycogenic ZnONPs.

3.3 FTIR

The FTIR spectra for ZnONPs synthesized from Trichoderma harzianum was observed in 4,000–500 cm^{-1} range. Peaks at 3,730 and 2,615 cm^{-1} suggested stretching of O–H bonds that resemble asymmetrical hydroxyl group which might be attributable to vibration of the surface hydroxyl group or adsorbed water. Another peak obtained at 2,345 cm^{-1} which showed the presence of CO_2 could be due to an instrumentation error. Peaks at 2,187 and 2,052 cm^{-1} confirmed the

presence of a carboxyl group. Peaks in the 1,600–1,000 cm^{-1} range revealed the existence of N compounds at 1,545 and 1024.2 cm^{-1} (Figure 3a). Furthermore two additional peaks were also observed in the 600–400 cm^{-1} range (663 and 401 cm^{-1}) indicating the stretching of the Zn–O atom [38].

3.4 XRD

The spectrum of ZnONPs, synthesized from *Trichoderma harzianum*, revealed different diffraction peaks at angles 31.7°, 34.3°, 36.2°, 47.4°, 56.5°, 62.80°, 66.3°, 67.8°, and 68.90° (Figure 3b). These peaks were further assigned to the planes associated with the Miller indices of (100), (002), (101), (102), (110), (103), (112), (201), and (004), respectively. All the peaks correspond to JCPDS card number 36-1451 and confirm the hexagonal wurtzite structure of ZnONPs [25].

3.5 SEM

SEM images clearly revealed the presence of distinct flower like morphology of the synthesized ZnONPs (Figure 4a and b). The SEM micrographs of myco-synthesized ZnONPs from *Trichoderma harzianum culture* filtrate was recorded in the range of 35–39 nm composed of many thin nanoscale petals radiating outwards from a central core in a flower shape. The smooth sheet like nanopetals with aligned facets give the appearance of a flower [39].

3.6 HR-TEM

The HR-TEM micrographs exhibited a flower pattern for ZnONPs ranging in size from 617 to 195 nm with an average size of 314 nm (Figure 4c and d). The flower-like ZnONPs displayed multiple, systematically arranged petals with petal size dimensions of an average of 100 nm length and 55 nm width. ZnO nanoflowers can be a result of flaky structures agglomerated in a polydisperse fashion. The agglomeration in the sample is due to the electrostatic attraction and polarity of synthesized mycogenic ZnONPs. The shape of ZnONPs can be altered by altering the reaction conditions [40].

3.7 EDX studies

The EDX studies of ZnONPs presented two peaks between 1 and 10 kV that are directly related to the absorption of the

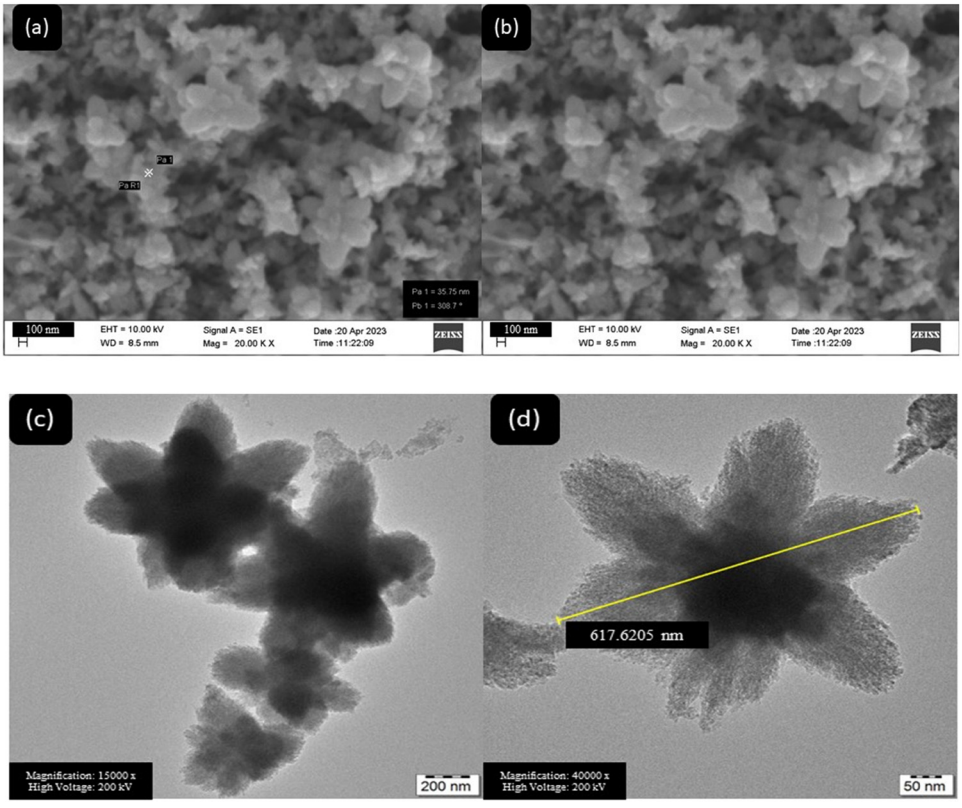

Figure 4: (a and b) SEM analysis and (c and d) TEM analysis of mycogenic ZnONPs at different magnifications.

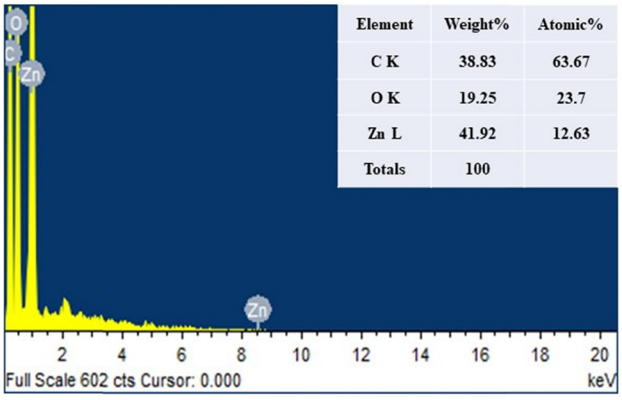

Figure 5: EDX analysis of mycogenic ZnONPs.

ZnONPs [41]. The results showed that the reaction product is made up of pure ZnONPs (Figure 5). The EDX weight composition revealed the presence of components such as copper (38.83%), oxygen (19.25%), and zinc (41.92%).

3.8 Analyzing the impact of different treatments of BS and ZnONPs formulation on *Vigna radiata* through *in vitro* experiments

The *in vitro* growth of the pre-soaked moong seeds with different treatments were finally evaluated after 5 days of incubation at 37°C for different parameters such as shoot length, root length, number of lateral roots, number of nodules, *etc.* There was a significant increase in the number of nodules and increase in lateral roots in the formulation F3 as compared to the control. Nodules are vital for biological nitrogen fixation enhancing legume productivity and soil fertility. Whereas lateral roots play a pivotal role in water and nutrient acquisition, anchorage, environmental adaptation, and vegetative propagation. It was concluded that ZnONPs in formulation with BS at an optimum concentration of 250 ppm were found to be the most effective by 22.6% as compared to the maintained control (Figure 6).

3.9 Analyzing the impact of different formulations of BS and ZnONPs on *Vigna radiata* through *in vivo* pot experiments

To analyze the impact of different formulations of BS and ZnONPs on *Vigna radiata*, pot experiments were designed in triplicates with different sets. Standard concentration of BS was used for the experiment. 1:2 ratio of ZnONPs and BS were used for the treatment. The results were evaluated on 30th and 60th day of sowing. Plant samples were uprooted and cleaned with distilled water for different phenological parameters measurement along with total phenol content and flavonoid content in the plant samples, chlorophyll content, *etc.*

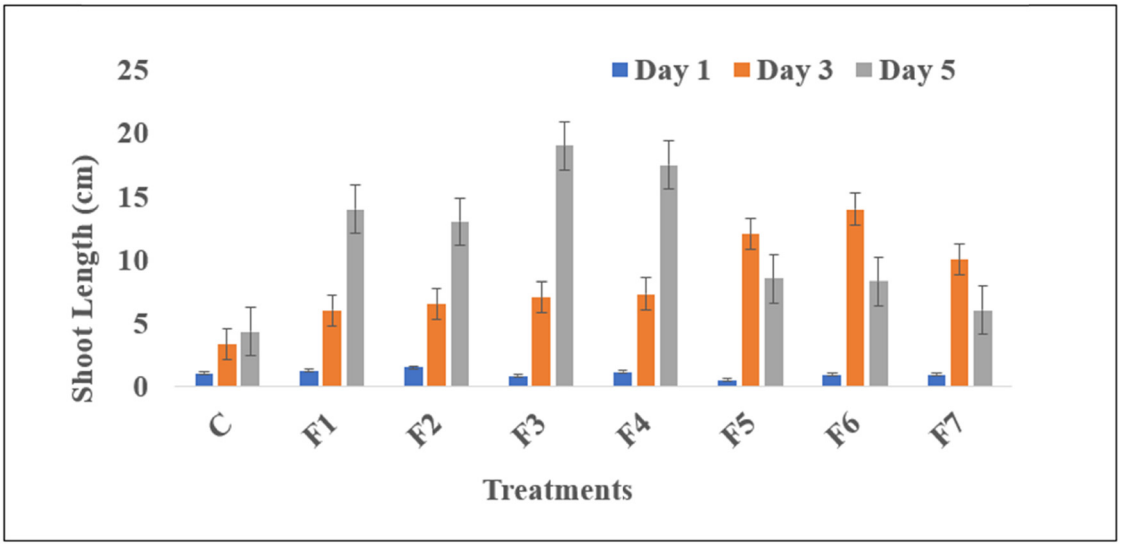

Figure 6: Effect of different formulations of BS and ZnONPs on physiological parameters of *Vigna Radiata* L (R) Wilczek (where C – control, F1 – BS + 1,000 ppm ZnONPs, F2 – BS + 500 ppm ZnONPs, F3 – BS + 250 ppm ZnONPs, F4 – BS + 200 ppm ZnONPs, F5 – BS + 100 ppm ZnONPs, F6 – BS + 50 ppm ZnONPs, and F7 – BS + 10 ppm ZnONPs).

3.10 Phenological parameters

After subjecting to different formulations, It was observed that in formulation (F3), the root length was maximum 11.4 ± 0.2 cm which is 75.3% increase in comparison to Control (C), which was 6.5 ± 0.2 cm at Day 30 and at Day 60 the root length was maximum with formulation (F3), 16.4 ± 0.4 cm which is 38.9% increase in comparison to control, which was 11.8 ± 0.05 cm (Figure 7a) and a similar pattern was observed for the shoot length at Day 30, and at Day 60 the shoot length was maximum for both the time period when treated with Formulation (F3). At day 30 the maximum shoot length was observed to be 31.3 ± 0.5 cm whereas at day 60 it increased to 47.06 ± 0.25 cm which is 45 % and 46.9% increase compared to Control as shown in Figure 7b.

3.11 Photosynthetic pigment analysis

Chlorophyll contents were estimated in order to access the effect of formulation of BS and different concentrations of ZnONPs on the photosynthetic pigments in mung bean plants. The chlorophyll content was measured after 30th

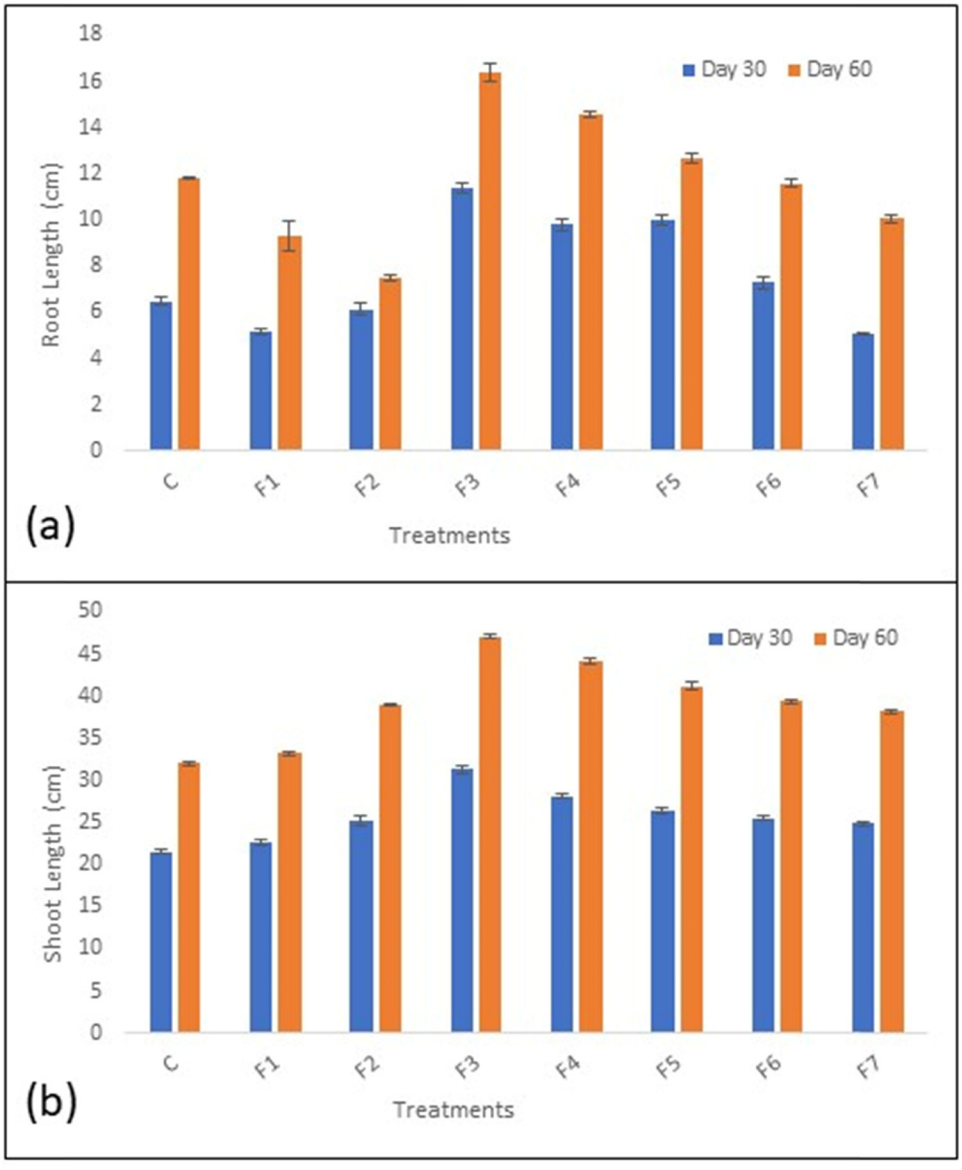

Figure 7: (a) Root length and (b) Shoot length of plants at Day 30 and Day 60 (where C –control, F1 – BS + 1,000 ppm ZnONPs, F2 – BS + 500 ppm ZnONPs, F3 – BS + 250 ppm ZnONPs, F4 – BS + 200 ppm ZnONPs, F5 – BS + 100 ppm ZnONPs, F6 – BS + 50 ppm ZnONPs, and F7 – BS + 10 ppm ZnONPs).

day and 60th day of sowing. Results indicated that there was no significant increase in treated plant samples as compared to control. Control (C) showed the maximum chlorophyll content, *i.e.*, 36.17 ± 0.1 mg/g at 30th day whereas the chlorophyll content showed uniformity in the treated samples after 60th day of sowing as shown in Figure 8a.

3.12 Estimation of flavonoid and phenol content

Phenolics and flavonoids are two major classes of plant secondary metabolites that possess antioxidant properties and are translocated to stressed areas to alleviate stress in plants [42]. At 30th day, phenolic compounds significantly lowered in formulation (F1), *i.e.*, from 289.43 ± 0.70 to 170.53 ± 0.52 in formulation (F2) but elevated thereafter in treated plants, but control showed the maximum value. But after 60th day, the treated leaf samples showed no significant increment in phenolic content in comparison to control but formulation (F2) showed the least increment 645 ± 0.8 GA/g (Figure 8b). However, flavonoids were also significantly higher in the treated samples but formulation (F4) showed the maximum of 100.91 ± 0.22 µg/g in contrast to control, *i.e.*, 25.08 ± 0.04 µg/g. But after 60 days, flavonoid content was lower in all the formulations except formulation (F6) (162.58 ± 0.7 µg/g) which showed the maximum content among all the formulation sets but was still lesser than the Control (167.02 ± 1.5 µg/g) (Figure 8c).

3.13 Discussion

The combined application of mycosynthesized ZnONPs and biogas plant slurry enhanced the agronomic performance of *Vigna radiata,* representing an advancement in agro nanotechnology. *Trichoderma harzianum* mediated green synthesis enables precise control over ZnONPs for agricultural applications. Characterization confirmed hexagonal wurtzite structure, 314 nm size, and 1.9 mV zeta potential. ZnONPs have been found to be a promising tool in renovating plant science by enhancing plant growth and productivity, functioning as a fertilizer, antimicrobial for disease management, and biosensors to monitor soil quality and plant health. ZnO NPs are known to promote plant growth by influencing plant hormone production, iron sequestration *via* siderophore, stress management *via* key enzymes such as 1-aminocyclopropane-1-carboxylate and soil organic matter decomposition [43–45]. However, the beneficial effects of ZnONPs on plant growth and yield vary with different plants as well as with the size and shape of ZnONPs. High doses and duration of exposure to ZnONPs can cause various detrimental effects in plants. ZnONPs can also induce the accumulation of reactive oxygen species and subsequent oxidative damage, thereby inhibiting plant growth [46]. However, low doses and duration of exposure to ZnONPs have been found to be beneficial in plants. Functionalization serves as an effective method to provide stability to the NPs, thereby reducing the harmful impact of ZnONPs in plants with the simultaneous

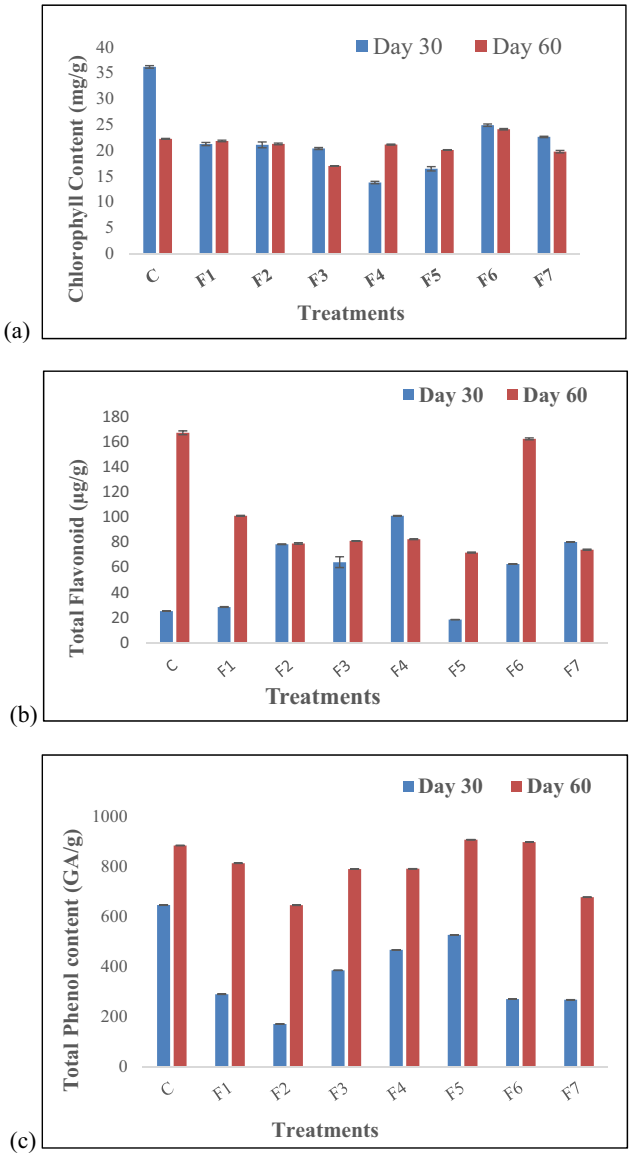

Figure 8: Analysis of (a) chlorophyll content, (b) total flavonoid content, (c) total phenolic content of different formulations (where C – control, F1 – BS + 1,000 ppm ZnONPs, F2– BS + 500 ppm ZnONPs, F3 – BS + 250 ppm ZnONPs, F4 – BS + 200 ppm ZnONPs, F5 – BS + 100 ppm ZnONPs, F6 – BS + 50 ppm ZnONPs, and F7 – BS + 10 ppm ZnONPs).

enhancement of efficacy. Unlike other metal oxide NPs, the ZnONPs does not induce phytotoxicity if used at optimal levels. Rather, synergistic interaction with BS stimulated growth [47]. This highlights the importance of optimizing NPs-BS formulations to leverage nanotechnology for sustainable agriculture [4]. The mechanism underlying enhanced germination and growth warrant investigation. Proposed hypotheses include: NPs increase nutrient availability, NPs modulate hormonal signaling, and NPs alleviate abiotic stress. Elucidating mechanisms will facilitate optimization of NPs-BS co-application for diverse crops and soils. Positive preliminary results motivate further research into prolonged impacts, environmental safety, and translational viability to boost crop yields sustainably. Overall, this nanobiofertilizers technology represents a promising tool for enhancing food production while advancing agricultural sustainability.

4 Conclusion

The study provides promising initial evidence that a nanobiofertilizer formulation combining BS and ZnONPs can enhance the growth of Vigna radiata plants. However, further research across multiple disciplines is needed to optimize the dosage, timing, and application methods; evaluate impacts on crop yield, soil health, secondary metabolites, and environmental sustainability; assess effectiveness in diverse soil types and crops, and determine feasibility for widespread use. Multidisciplinary field trials, biochemical analyses, agronomic studies, and cost-benefit assessments can provide valuable insights to translate this technology into eco-friendly agricultural practices. Overall, this study indicates the potential of nanobiofertilizers to improve crop productivity, but more expansive research is required to fully understand the short and long-term impacts before commercialization.

Acknowledgments: The authors would like to thank Professor Ajit Varma (Distinguished Scientist and Professor of Eminence, Amity Institute of Microbial Technology) for providing them lab facility for the completion of this work.

Funding information: The authors state no funding involved.

Author contributions: Abhinav Singh, Ram Prasad, and Arti Goel contributed to the study conception and design. Material preparation, data collection, and analysis were performed by Abhinav Singh. Ajit Varma provided the necessary lab equipment and chemicals required in the study. Arti Goel, Sharanagouda Hiregoudar, Ritika Chauhan, and Ram Prasad helped in analysis, writing, and editing the manuscript. The first draft of the manuscript was written by Abhinav Singh. All authors have accepted responsibility for the entire content of this manuscript and approved its submission.

Conflict of interest: The authors state no conflict of interest.

References

[1] Khazaei H, Subedi M, Nickerson M, Martínez-Villaluenga C, Frias J, Vandenberg A. Seed protein of lentils: Current status, progress, and food applications. Foods. 2019;8(9):391.

[2] Kchaou R, Benyoussef S, Jebari S, Harbaoui K, Berndtsson R. Forage potential of cereal–legume mixtures as an adaptive climate change strategy under low input systems. Sustainability. 2022;15(1):338.

[3] Popoola JO, Ojuederie OB, Aworunse OS, Adelekan A, Oyelakin AS, Oyesola OL, et al. Nutritional, functional, and bioactive properties of African underutilized legumes. Front Plant Sci. 2023;14:1105364.

[4] Farooq MS, Uzair M, Raza A, Habib M, Xu Y, Yousuf M, et al. Uncovering the research gaps to alleviate the negative impacts of climate change on food security: A review. Front Plant Sci. 2022;13:927535.

[5] Chaudhary P, Chaudhary A, Bhatt P, Kumar G, Khatoon H, Rani A, et al. Assessment of soil health indicators under the influence of nanocompounds and Bacillus spp. in field condition. Front Environ Sci. 2022;9:769871.

[6] Singh N, Singh R, Shah K, Pramanik BK. Green synthesis of zinc oxide nanoparticles using lychee peel and its application in antibacterial properties and CR dye removal from wastewater. Chemosphere. 2023;327:138497.

[7] Kumar A, Verma LM, Sharma S, Singh N. Overview on agricultural potentials of biogas slurry (BGS): Applications, challenges, and solutions. Biomass Convers Biorefin. 2022;13:1–41.

[8] Sánchez-López E, Gomes D, Esteruelas G, Bonilla L, Lopez-Machado AL, Galindo R, et al. Metal-based nanoparticles as antimicrobial agents: an overview. Nanomaterials. 2020;10(2):292.

[9] Mdlambuzi T, Tsubo M, Muchaonyerwa P. Short-term effects of selected organic fertilizer sources on carbon dioxide fluxes and soil quality. J Environ Qual. 2021;50:312–23.

[10] Raha S, Ahmaruzzaman M. ZnO nanostructured materials and their potential applications: progress, challenges and perspectives. Nanoscale Adv. 2022;4(8):1868–925.

[11] Hidangmayum A, Debnath A, Guru A, Singh BN, Upadhyay SK, Dwivedi P. Mechanistic and recent updates in nano-bioremediation for developing green technology to alleviate agricultural contaminants. Int J Environ Sci Technol. 2023;20(10):11693–718.

[12] Foroozandeh P, Aziz AA. Insight into cellular uptake and intracellular trafficking of nanoparticles. Nanoscale Res Lett. 2018;13:1–12.

[13] Kebede T, Keneni YG, Senbeta AF, Sime G. Effect of bioslurry and chemical fertilizer on the agronomic performances of maize. Heliyon. 2023;9(1):e13000.

[14] de Matos Nascimento A, Maciel AM, Silva JBG, Mendonça HV, de Paula VR, Otenio MH. Biofertilizer application on corn (Zea mays)

increases the productivity and quality of the crop without causing environmental damage. Water Air Soil Pollut. 2020;231:1–10.
[15] Shamoradi F, Marashi SK. Influence of chemical and biological fertilizers on agro-physiological characteristics of corn (*Zea mays* L., SC 703). J Crop Nutr Sci. 2018;4(1):1–16.
[16] Gao C, El-Sawah AM, Ali DF, Alhaj Hamoud Y, Shaghaleh H, Sheteiwy MS. The integration of bio and organic fertilizers improve plant growth, grain yield, quality and metabolism of hybrid maize (*Zea mays* L.). Agronomy. 2020;10:319.
[17] Almaghasla MI, El-Ganainy SM, Ismail AM. Biological activity of four *Trichoderma* species confers protection against *Rhizoctonia solani*, the causal agent of cucumber damping-off and root rot diseases. Sustainability. 2023;15:7250.
[18] Ahmed T, Luo J, Noman M, Ijaz M, Wang X, Masood HA, et al. Microbe-mediated nanoparticle intervention for the management of plant diseases. Crop Heal. 2023;1(1):3.
[19] Soesanto L, Fakhiroh Z, Suharti WS. Viability and virulence of *Fusarium oxysporum f. sp.* zingiberi isolates from Boyolali and Temanggung preserved for 17 years in sterile soils. J Fitopatol Indones. 2022;18(2):91–9.
[20] Shobha B, Ashwini BS, Ghazwani M, Hani U, Atwah B, Alhumaidi MS, et al. Trichoderma-mediated ZnO nanoparticles and their antibiofilm and antibacterial activities. J Fungi. 2023;9(2):133.
[21] Fernández-Pérez A, Marbán G. Room temperature sintering of polar ZnO nanosheets: III-Prevention. Microporous Mesoporous Mater. 2020;294:109836.
[22] Gholami M, Esmaeilzadeh M, Kachoei Z, Kachoei M, Divband B. Influence of physical dimension and morphological-dependent antibacterial characteristics of ZnO nanoparticles coated on orthodontic NiTi wires. Biomed Res Int. 2021;2021:6397698.
[23] Dhiman S, Singh S, Varma A, Goel A. Phytofabricated zinc oxide nanoparticles as a nanofungicide for management of Alternaria blight of Brassica. BioMetals. 2021;34:1275–93.
[24] Gharpure S, Yadwade R, Ankamwar B. Non-antimicrobial and Non-anticancer properties of ZnO nanoparticles biosynthesized using different plant parts of Bixa orellana. ACS Omega. 2022 Jan;7(2):1914–33.
[25] Ashwini J, Aswathy TR, Rahul AB, Thara GM, Nair AS. Synthesis and characterization of zinc oxide nanoparticles using *Acacia caesia* bark extract and its photocatalytic and antimicrobial activities. Catalysts. 2021;11(12):1507.
[26] Shaikhaldein HO, Al-Qurainy F, Khan S, Nadeem M, Tarroum M, Salih AM, et al. Biosynthesis and characterization of ZnO nanoparticles using *ochradenus arabicus* and their effect on growth and antioxidant systems of *Maerua oblongifolia*. Plants. 2021;10(9):1808.
[27] Loganathan S, Shivakumar MS, Karthi S, Nathan SS, Selvam K. Metal oxide nanoparticle synthesis (ZnO-NPs) of *Knoxia sumatrensis* (Retz.) DC. Aqueous leaf extract and it's evaluation of their antioxidant, anti-proliferative and larvicidal activities. Toxicol Rep. 2021;8:64–72.
[28] Song Z, Kelf TA, Sanchez WH, Roberts MS, Rička J, Frenz M, et al. Characterization of optical properties of ZnO nanoparticles for quantitative imaging of transdermal transport. Biomed Opt Express. 2011;2(12):3321–33.
[29] Song P, Zhao B, Sun X, Li L, Wang Z, Ma C, et al. Effects of Bacillus subtilis HS5B5 on maize seed germination and seedling growth under NaCl stress conditions. Agronomy. 2023;13(7):1874.
[30] Rawashdeh RY, Harb AM, AlHasan AM. Biological interaction levels of zinc oxide nanoparticles; lettuce seeds as case study. Heliyon. 2020;6(5):e03983.
[31] Hameed H, Waheed A, Sharif MS, Saleem M, Afreen A, Tariq M, et al. Green synthesis of zinc oxide (ZnO) nanoparticles from green algae and their assessment in various biological applications. Micromachines. 2023 Apr;14(5):928.
[32] Singh CM, Singh P, Tiwari C, Purwar S, Kumar M, Pratap A, et al. Improving drought tolerance in mung bean (Vigna radiata L. Wilczek): morpho-physiological, biochemical and molecular perspectives. Agronomy. 2021;11(8):1534.
[33] Saleem MH, Ali S, Kamran M, Iqbal N, Azeem M, Tariq Javed M, et al. Ethylenediaminetetraacetic acid (EDTA) mitigates the toxic effect of excessive copper concentrations on growth, gaseous exchange and chloroplast ultrastructure of *Corchorus capsularis L.* and improves copper accumulation capabilities. Plants. 2020;9(6):756.
[34] Aminot A, Rey F. Standard procedure for the determination of chlorophyll a by spectroscopic methods. Int Counc Explor Sea. 2000;112:25.
[35] Zhishen J, Mengcheng T, Jianming W. The determination of flavonoid contents in mulberry and their scavenging effects on superoxide radicals. Food Chem. 1999;64(4):555–9.
[36] Karam ST, Abdulrahman AF. Green synthesis and characterization of ZnO nanoparticles by using thyme plant leaf extract. Photonics. 2022;9:594.
[37] Tymoszuk A, Wojnarowicz J. Zinc oxide and zinc oxide nanoparticles impact on in vitro germination and seedling growth in *Allium cepa L*. Materials (Basel). 2020;13(12):2784.
[38] Hossain A, Abdallah Y, Ali MA, Masum MMI, Li B, Sun G, et al. Lemon-fruit-based green synthesis of zinc oxide nanoparticles and titanium dioxide nanoparticles against soft rot bacterial pathogen *Dickeya dadantii*. Biomolecules. 2019;9(12):863.
[39] Mohd Yusof H, Abdul Rahman N, Mohamad R, Zaidan UH, Samsudin AA. Biosynthesis of zinc oxide nanoparticles by cell-biomass and supernatant of *Lactobacillus plantarum* TA4 and its antibacterial and biocompatibility properties. Sci Rep. 2020;10(1):19996.
[40] Zaki SA, Ouf SA, Albarakaty FM, Habeb MM, Aly AA, Abd-Elsalam KA. Trichoderma harzianum-mediated ZnO nanoparticles: A green tool for controlling soil-borne pathogens in cotton. J Fungi. 2021;7(11):952.
[41] Demissie MG, Sabir FK, Edossa GD, Gonfa BA. Synthesis of zinc oxide nanoparticles using leaf extract of *Lippia adoensis* (Koseret) and evaluation of its antibacterial activity. J Chem. 2020;2020:9.
[42] Mutha RE, Tatiya AU, Surana SJ. Flavonoids as natural phenolic compounds and their role in therapeutics: An overview. Futur J Pharm Sci. 2021;7:1–13.
[43] Sun L, Wang R, Ju Q, Xing M, Li R, Li W, et al. Mitigation mechanism of zinc oxide nanoparticles on cadmium toxicity in tomato. Front Plant Sci. 2023;14:1162372.
[44] Thounaojam TC, Meetei TT, Devi YB, Panda SK, Upadhyaya H. Zinc oxide nanoparticles (ZnO-NPs): a promising nanoparticle in renovating plant science. Acta Physiol Plant. 2021;43:1–21.
[45] Wang X, Xie H, Wang P, Yin H. Nanoparticles in plants: Uptake, transport and physiological activity in leaf and root. Materials (Basel). 2023;16(8):3097.
[46] Yu Z, Li Q, Wang J, Yu Y, Wang Y, Zhou Q, et al. Reactive oxygen species-related nanoparticle toxicity in the biomedical field. Nanoscale Res Lett. 2020;15(1):115.
[47] Shobha B, Lakshmeesha TR, Ansari MA, Almatroudi A, Alzohairy MA, Basavaraju S, et al. Mycosynthesis of ZnO nanoparticles using Trichoderma spp. isolated from rhizosphere soils and its synergistic antibacterial effect against *Xanthomonas oryzae pv. oryzae*. J Fungi. 2020;6(3):181.